

## Quantum Fluctuations and Magnetic Structures of $\text{CsCuCl}_3$ in High Magnetic Field

Tetsuro NIKUNI and Hiroyuki SHIBA

*Department of Physics, Tokyo Institute of Technology,  
Oh-okayama, Tokyo 152*

(Received April 28, 1993)

A theoretical interpretation is given on the magnetization process of  $\text{CsCuCl}_3$  showing a small jump for the external field applied parallel to the  $c$ -axis. It is shown that quantum fluctuations are so important in this  $S=1/2$  triangular antiferromagnet that they can change the ground-state spin structure. The observed magnetization jump is successfully explained as a spin flop process caused by the quantum effect.

### §1. Introduction

$\text{CsCuCl}_3$  is one of the well-known hexagonal  $\text{ABX}_3$ -type compounds which has been extensively investigated.<sup>1–6</sup> It is featured by the ferromagnetic chains along the  $c$ -axis which form the triangular antiferromagnet in the  $c$ -plane. It undergoes a structural phase transition at 423 K leading to a helical atomic displacement along the  $c$ -axis. This is attributed to the cooperative Jahn-Teller effect of  $\text{Cu}^{2+}$  ion.<sup>7</sup> The low symmetry of the local structure leads to the antisymmetric Dzyaloshinsky-Moriya (D-M) interaction along the chains. Below  $T_N=10.5$  K, spins lie on the  $c$ -plane with the  $120^\circ$  structure and form a helical spin structure along the  $c$ -axis with a long period.<sup>1)</sup> The helical structure is explained by a competition between the ferromagnetic intrachain exchange interaction and the D-M interaction.

In a high field experiment, Motokawa<sup>8)</sup> discovered an unexpected behavior in magnetization process of  $\text{CsCuCl}_3$ . When the external field is applied parallel to the  $c$ -axis, the magnetization at  $T=1.1$  K increases almost linearly and shows a small jump at  $H_c=12.5$  T. Above  $H_c$ , the magnetization increases again and saturates at  $H_s=31$  T. According to the classical mean-field theory, spins should simply stand up from the  $c$ -plane so as to form the umbrella-like spin structure (Fig. 1(a)), when the field is applied along the  $c$ -axis. The umbrella closes continuously with increasing

field, and finally shrinks into the ferromagnetic state. Thus, it is difficult to explain the observed magnetization jump within the classical theory.

In most magnetic substances, their spin structures are well determined within the classical theory. It is generally believed therefore that quantum fluctuations do not change the nature of the ground state of real (three-dimensional) magnets. However there are some exceptions for frustrated systems. It is known theoretically that frustrated spin systems often show non-trivial continuous degeneracy in the classical ground state. Such a degeneracy is usually removed by thermal or quantum fluctuations. The triangular antiferromagnet in a magnetic field,<sup>8–10)</sup> the fcc Heisenberg antiferromagnet,<sup>11)</sup> and a frustrated square-lattice antiferromagnet<sup>12)</sup> are such examples. However no real material has been known up to now.

The purpose of the present paper is to show that  $\text{CsCuCl}_3$  is the first material in which quantum fluctuations play an important role in determining the ground state spin structure. We will show that the unexpected behavior of the magnetization is a manifestation of quantum fluctuations.

A preliminary account of a part of this work was reported in ref. 13.

### §2. Classical Ground State

Let us write the Hamiltonian of  $\text{CsCuCl}_3$  in the magnetic field applied parallel to the  $c$ -axis as

$$\begin{aligned} \mathcal{H} = & -2J_0 \sum_{in} (S_{in} \cdot S_{in+1} + \eta (S_{in}^x S_{in+1}^x + S_{in}^y S_{in+1}^y)) + 2J_1 \sum_{\langle ij \rangle_n} S_{in} \cdot S_{jn} \\ & - \sum_{in} \mathbf{D}_{nn+1} \cdot (S_{in} \times S_{in+1}) - g\mu_B H \sum_{in} S_{in}^z, \end{aligned} \quad (1)$$

where  $S_{in}$  represents a spin ( $S=1/2$ ) located at the  $i$ -th site in the  $n$ -th  $c$ -plane, and the summation  $\langle ij \rangle$  is taken over all nearest-neighbor pairs in the  $c$ -plane. The  $z$ -axis is taken to be parallel to the  $c$ -axis. The first and second terms are intrachain ferromagnetic exchange interaction and interchain antiferromagnetic exchange interaction, respectively.  $\eta (>0)$  is a weak anisotropic exchange interaction of easy-plane type, whose importance has been pointed out by Tanaka *et al.*<sup>5)</sup> The third term is the D-M interaction where the  $\mathbf{D}_{nn+1}$  vector is assumed to be parallel to the  $c$ -axis. The fourth term is the Zeeman energy. The dipole-dipole interaction is considered to be small and neglected for simplicity.

Although the Hamiltonian (1) looks complicated due to the D-M interaction, we can eliminate the asymmetric part from the Hamiltonian by rotating the  $xy$ -plane by a pitch  $q$  along the  $z$ -axis as

$$\begin{cases} S_{in}^x = S_{in}^{x'} \cos nq - S_{in}^{y'} \sin nq, \\ S_{in}^y = S_{in}^{x'} \sin nq + S_{in}^{y'} \cos nq. \end{cases} \quad (2)$$

The Hamiltonian is then written as

$$\mathcal{H} = - \sum_{in} [2\tilde{J}_0 (S_{in}^x S_{in+1}^x + S_{in}^y S_{in+1}^y) + 2J_0 S_{in}^z S_{in+1}^z] + 2J_1 \sum_{\langle ij \rangle_n} S_{in} \cdot S_{jn} - g\mu_B H \sum_{in} S_{in}^z, \quad (3)$$

where

$$\tilde{J}_0 = J_0 \sqrt{(1+\eta)^2 + \left(\frac{D}{2J_0}\right)^2}, \quad D \equiv |D_{nn+1}^z|. \quad (4)$$

We omitted the notation “ ’ ” in (2) for simplicity. The pitch  $q$  of the helical structure is determined so as to eliminate the asymmetric term:  $\tan q = D/2J_0(1+\eta)$ . According to experimental results,<sup>5)</sup>  $\tilde{J}_0$  is estimated as  $\tilde{J}_0 = 1.012J_0$ . Note that the antisymmetric interaction has been reduced to a weak anisotropy of easy-plane type.

In the classical ground state the triangular antiferromagnet on each  $c$ -plane can be divided into 3 sublattices labeled by 1, 2, 3. The ground state energy is described with the spin of the  $l$ -th sublattice  $S_l$  as

$$\begin{aligned} \frac{E_0}{N} = & -2\tilde{J}_0 S^2 + \frac{2}{3} (\tilde{J}_0 - J_0) \{ (S_1^z)^2 + (S_2^z)^2 + (S_3^z)^2 \} \\ & + 2J_1 (S_1 \cdot S_2 + S_2 \cdot S_3 + S_3 \cdot S_1) - \frac{1}{3} g\mu_B H (S_1^z + S_2^z + S_3^z), \end{aligned} \quad (5)$$

where  $N$  represents the total number of spins. It is convenient to express  $S_l$  with the polar coordinate as

$$S_l = (S \cos \phi_l \sin \theta_l, S \sin \phi_l \sin \theta_l, S \cos \theta_l) \quad (6)$$

We shall consider the four types of spin configurations shown in Fig. 1, which are possible candidates for the ground state.

[I] umbrella-type configuration (Fig. 1(a))

This configuration is expected to be the ground-state configuration in the classical theory. Putting  $\theta_l \equiv \theta$  and  $\phi_l = 2(l-1)\pi/3$ , we have the classical energy of this configuration as

$$\frac{E_0}{N} = -2\tilde{J}_0 S^2 - 3J_1 S^2 + \{2(\tilde{J}_0 - J_0) + 9J_1\} S^2 \cos^2 \theta - g\mu_B H S \cos \theta. \quad (7)$$

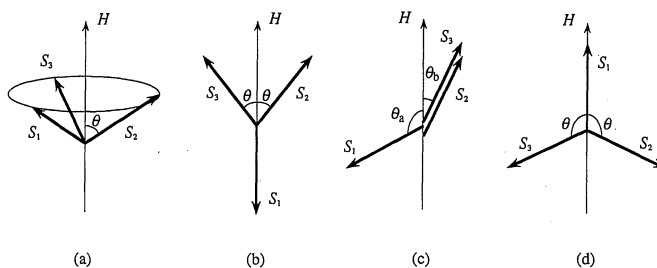


Fig. 1. Four types of spin configurations of the triangular antiferromagnet in the magnetic field. (a) The umbrella-type configuration. The  $c$ -plane components of the spins form the  $120^\circ$  structure. (b) The coplanar configuration for  $H < H_s/3$ . The spins lie in a plane including the  $c$ -axis. (c) The coplanar configuration for  $H > H_s/3$ . Two of the three spins are oriented along the same direction. (d) The coplanar configuration, which is the inversion of the configuration (b).

The angle  $\theta$  is determined by the condition  $\partial E_0/\partial \theta = 0$ , which leads to

$$\cos \theta = \frac{g \mu_B H}{(18 + 4\Delta) J_1 S}, \quad (8)$$

where  $\Delta \equiv (\tilde{J}_0 - J_0)/J_1$ . The magnetization is given by  $M = g \mu_B S \cos \theta$ . The magnetization shows a linear increase with the increase of the external field and then it saturates at

$$H_s = (18 + 4\Delta) J_1 S / g \mu_B. \quad (9)$$

Substituting (8) into (7), we have the minimum energy of this configuration as

$$\frac{E_0}{N} = -(2\tilde{J}_0 + 3J_1)S^2 - \frac{1}{2} g \mu_B S H_s h^2, \quad (10)$$

where  $h = H/H_s$ .

## [II] coplanar configurations

To describe the coplanar configurations, we put  $\phi_1 = \phi_2 = \phi_3 = 0$  and take  $\theta_i$  between  $-\pi$  and  $\pi$ . We consider three types of coplanar configurations.

(i)  $\theta_1 = \pi$  and  $\theta_2 = -\theta_3 \equiv \theta$  (Fig. 1(b))

For this configuration, the classical energy is

$$\frac{E_0}{N} = -2\tilde{J}_0 S^2 + \frac{2}{3} (\tilde{J}_0 - J_0) S^2 (1 + 2 \cos^2 \theta) + 2J_1 S^2 (\cos 2\theta - 2 \cos \theta) - \frac{1}{3} g \mu_B S H (2 \cos \theta - 1). \quad (11)$$

The angle  $\theta$  is determined by minimizing (11), which leads to

$$\cos \theta = \frac{(g \mu_B H/S) + 6J_1}{(12 + 4\Delta) J_1}. \quad (12)$$

The minimum energy for this configuration is obtained by substituting (12) into (11). Since  $\Delta$  is estimated to be  $\approx 0.07$  for  $\text{CsCuCl}_3$ , we expand the energy with respect to  $\Delta$  as

$$\frac{E_0}{N} = -(2\tilde{J}_0 + 3J_1)S^2 - \frac{1}{2} g \mu_B S H_s h^2 + \Delta J_1 (1 + h)^2 S^2 + O(\Delta^2). \quad (13)$$

The third term of the above equation is the energy difference from the umbrella configuration. This term is always positive for  $\Delta > 0$ .

(ii)  $\theta_1 = -\theta_a$  and  $\theta_2 = \theta_3 = \theta_b$  (Fig. 1(c))

The classical energy of this configuration is

$$\begin{aligned} \frac{E_0}{N} = & -2\tilde{J}_0 S^2 + \frac{2}{3} (\tilde{J}_0 - J_0) S^2 (\cos^2 \theta_a + 2 \cos^2 \theta_b) \\ & + 2J_1 S^2 \{1 + 2 \cos(\theta_a + \theta_b)\} - \frac{1}{3} g\mu_B SH (\cos \theta_a + 2 \cos \theta_b). \end{aligned} \quad (14)$$

From the conditions  $\partial E_0 / \partial \theta_a = 0$  and  $\partial E_0 / \partial \theta_b = 0$ , the following two equations are obtained:

$$\begin{cases} \Delta \sin 2\theta_a + 6 \sin(\theta_a + \theta_b) - (9 + 2\Delta) h \sin \theta_a = 0, \\ \Delta \sin 2\theta_b + 3 \sin(\theta_a + \theta_b) - (9 + 2\Delta) h \sin \theta_b = 0. \end{cases} \quad (15)$$

For  $\Delta \neq 0$ , it is difficult to solve (15) for a general case. However, for small  $\Delta$ , we can express  $\cos \theta_a$  and  $\cos \theta_b$  as an expansion in  $\Delta$  as

$$\begin{cases} \cos \theta_a = \frac{3}{2} h - \frac{1}{2h} + \Delta \frac{(1-h^2)(7-3h^2)}{36h^2} + O(\Delta^2), \\ \cos \theta_b = \frac{3}{4} h + \frac{1}{4h} - \Delta \frac{(1-h^2)(2-3h^2)}{36h^2} + O(\Delta^2). \end{cases} \quad (16)$$

Substituting (16) into (14), we obtain the energy of this configuration up to the first order in terms of  $\Delta$  as

$$\frac{E_0}{N} = -(2\tilde{J}_0 + 3J_1) S^2 - \frac{1}{2} g\mu_B SH_s h^2 + \Delta J_1 S^2 \frac{(1-h^2)^2}{4h^2} + O(\Delta^2). \quad (17)$$

We find that for positive  $\Delta$ , this energy is higher than that in the umbrella-type.

(iii)  $\theta_1 = \pi$ ,  $\theta_2 = -\theta_3 \equiv \theta$  (Fig. 1(d))

The classical energy for this configuration is,

$$\frac{E_0}{N} = -2\tilde{J}_0 S^2 + \frac{2}{3} (\tilde{J}_0 - J_0) S^2 (1 + 2 \cos^2 \theta) + 2J_1 S^2 (\cos 2\theta + 2 \cos \theta) - \frac{1}{3} g\mu_B SH (2 \cos \theta + 1). \quad (18)$$

The angle  $\theta$  is determined from the condition  $\partial E_0 / \partial \theta$ , which leads to

$$\cos \theta = \frac{(g\mu_B H / S) - 6J_1}{(12 + 4\Delta) J_1}. \quad (19)$$

The minimum energy for this configuration is obtained by substituting (19) into (18) as

$$\frac{E_0}{N} = -(2\tilde{J}_0 + 3J_1) S^2 - \frac{1}{2} g\mu_B SH_s h^2 + \Delta J_1 (1-h)^2 S^2 + O(\Delta^2). \quad (20)$$

Although this energy is lower than that of the configuration (b) or (c), it is still higher than the energy of the umbrella-type.

Actually, all configurations shown above satisfy the relation

$$S_1 + S_2 + S_3 = \frac{g\mu_B H}{6J_1}, \quad (21)$$

for  $\Delta = 0$  and they all belong to the class of continuously degenerate ground states.<sup>9)</sup> For  $\Delta > 0$ , the continuous degeneracy is removed by the easy-plane anisotropy and the umbrella-type configuration is selected as the ground state. Note that the energy difference between coplanar and umbrella-type is very small for small  $\Delta$ . Thus we expect that the energy difference can be compensated by the effect of quantum fluctuations, as will be shown explicitly in the next section.

### §3. Quantum Fluctuations

In this section we take into account the effect of quantum fluctuations by means of the spin-

wave theory. This gives the first correction to the classical ground state energy in the  $1/S$  expansion. We evaluate the zero-point energy for the four spin configurations by putting  $\Delta=0$ , and see how quantum fluctuations lift the degeneracy of the classical state in the isotropic case.

We take a local coordinate system  $\xi, \eta, \zeta$  in which the  $\zeta$ -axis is taken to be the classical direction of the spin. The transformation in each sublattice is expressed in terms of the polar coordinate of the classical direction as

$$\begin{cases} S_{in}^x = -S_{in}^\xi \sin \phi_l - S_{in}^\eta \cos \theta_l \cos \phi_l + S_{in}^\zeta \sin \theta_l \cos \phi_l, \\ S_{in}^y = S_{in}^\xi \cos \phi_l - S_{in}^\eta \cos \theta_l \sin \phi_l + S_{in}^\zeta \sin \theta_l \sin \phi_l, \\ S_{in}^z = S_{in}^\eta \sin \theta_l + S_{in}^\zeta \cos \theta_l, \end{cases} \quad (22)$$

where the angles  $\theta_l$  and  $\phi_l$  have already been determined for each configuration classically. We introduce three kinds of Holstein-Primakoff bosons  $a, b, c$  for the sublattice 1, 2, 3 respectively. The spin deviation from the classical direction on the 1st sublattice is described then by the bosonic operator as

$$S_{in}^\zeta = S - a_{in}^\dagger a_{in}, \quad S_{in}^\xi = \frac{\sqrt{2S}}{2} (a_{in}^\dagger + a_{in}), \quad S_{in}^\eta = i \frac{\sqrt{2S}}{2} (a_{in}^\dagger - a_{in}). \quad (23)$$

For the other sublattices, the bosonic operators are defined in the same way as in (23). The Fourier transform of the bosonic operator is defined by

$$a_{in} = \sqrt{\frac{3}{N}} \sum_k a_k \exp(i\mathbf{k} \cdot \mathbf{r}_{in}), \quad (24)$$

where the wave vector  $\mathbf{k}$  is defined in the Brillouin zone for the sublattice. Substituting these operators into the Hamiltonian and neglecting terms higher than the third order in bosonic operators according to the spirit of the  $1/S$  expansion, we obtain a quadratic spin-wave Hamiltonian as

$$\mathcal{H}_{\text{sw}} = E_0 - (2J_0 + 3J_1)NS + \frac{S}{2} \sum_k \left[ (\mathcal{A}_k^\dagger, \mathcal{A}_{-k}) \begin{pmatrix} E_k & F_k \\ F_{-k}^* & E_{-k}^* \end{pmatrix} \begin{pmatrix} \mathcal{A}_k \\ \mathcal{A}_{-k}^\dagger \end{pmatrix} \right], \quad (25)$$

where  $\mathcal{A}_k$  is a three-component vector  $\mathcal{A}_k = (a_k, b_k, c_k)$ , and  $E_k$  and  $F_k$  are  $3 \times 3$  matrices. The matrix elements of  $E$  and  $F$  are

$$\begin{cases} E_{11} = E_{22} = E_{33} = 4J_0(1 - \cos k_z) + 6J_1, \\ E_{12} = E_{21}^* = 3J_1 \{ (1 + \cos \theta_1 \cos \theta_2) \cos(\phi_1 - \phi_2) + \sin \theta_1 \sin \theta_2 \\ \quad - i(\cos \theta_1 + \cos \theta_2) \sin(\phi_1 - \phi_2) \} v_k, \\ E_{23} = E_{32}^* = 3J_1 \{ (1 + \cos \theta_2 \cos \theta_3) \cos(\phi_2 - \phi_3) + \sin \theta_2 \sin \theta_3 \\ \quad - i(\cos \theta_2 + \cos \theta_3) \sin(\phi_2 - \phi_3) \} v_k, \\ E_{31} = E_{13}^* = 3J_1 \{ (1 + \cos \theta_3 \cos \theta_1) \cos(\phi_3 - \phi_1) + \sin \theta_3 \sin \theta_1 \\ \quad - i(\cos \theta_3 + \cos \theta_1) \sin(\phi_3 - \phi_1) \} v_k, \end{cases} \quad (26)$$

$$\begin{cases} F_{11} = F_{22} = F_{33} = 0, \\ F_{12} = F_{21}^* = 3J_1 \{ (1 - \cos \theta_1 \cos \theta_2) \cos(\phi_1 - \phi_2) - \sin \theta_1 \sin \theta_2 \\ \quad - i(\cos \theta_1 - \cos \theta_2) \sin(\phi_1 - \phi_2) \} v_k, \\ F_{23} = F_{32}^* = 3J_1 \{ (1 - \cos \theta_2 \cos \theta_3) \cos(\phi_2 - \phi_3) - \sin \theta_2 \sin \theta_3 \\ \quad - i(\cos \theta_2 - \cos \theta_3) \sin(\phi_2 - \phi_3) \} v_k, \\ F_{31} = F_{13}^* = 3J_1 \{ (1 - \cos \theta_3 \cos \theta_1) \cos(\phi_3 - \phi_1) - \sin \theta_3 \sin \theta_1 \\ \quad - i(\cos \theta_3 - \cos \theta_1) \sin(\phi_3 - \phi_1) \} v_k, \end{cases} \quad (27)$$

where

$$v_k = \frac{1}{3} \left[ \exp(ik_x) + \exp \left\{ i \left( \frac{-k_x + \sqrt{3} k_y}{2} \right) \right\} + \exp \left\{ i \left( \frac{-k_x - \sqrt{3} k_y}{2} \right) \right\} \right]. \quad (28)$$

The Hamiltonian  $\mathcal{H}_{\text{SW}}$  is diagonalized by a generalized Bogoliubov transformation which results in

$$\begin{aligned} \mathcal{H}_{\text{SW}} = E_0 - (2J_0 + 3J_1)NS + S \sum_k & \left[ \omega_1(k) \left( \alpha_k^\dagger \alpha_k + \frac{1}{2} \right) \right. \\ & \left. + \omega_2(k) \left( \beta_k^\dagger \beta_k + \frac{1}{2} \right) + \omega_3(k) \left( \gamma_k^\dagger \gamma_k + \frac{1}{2} \right) \right]. \end{aligned} \quad (29)$$

Therefore the first quantum correction to the classical ground state energy for each spin configuration is given by

$$\Delta E_{\text{SW}} = -(2J_0 + 3J_1)NS + \frac{S}{2} \sum_k [\omega_1(k) + \omega_2(k) + \omega_3(k)], \quad (30)$$

as expected.

For the umbrella-type configuration, the diagonalization of the Hamiltonian can be easily carried out. The spin-wave energy  $\omega_l(k)$  is given by

$$\begin{aligned} \omega_l(k) = & \sqrt{[4J_0(1 - \cos k_z) + 6J_1(1 - \lambda_{l,k})][4J_0(1 - \cos k_z) + 6J_1\{1 + (2 - 3h^2)\lambda_{l,k}\}]} \\ & - 6\sqrt{3} J_1 h \mu_{l,k}. \end{aligned} \quad (31)$$

where  $\lambda_{l,k} = \{j^{(l-1)}v_k + j^{-(l-1)}v_{-k}\}/2$  and  $\mu_{l,k} = \{j^{(l-1)}v_k - j^{-(l-1)}v_{-k}\}/2i$  with  $j = e^{i2\pi/3}$ .

For the coplanar configurations,  $\omega_l(k)$  is given by the solution of

$$\det[(E - F)(E + F) - \omega^2] = 0. \quad (32)$$

Although it is difficult to write the solution in an explicit form for arbitrary wave vector  $k$ , spin-wave frequencies can be determined by solving (32) numerically. The spin-wave frequencies, which were calculated for the umbrella-type configuration in Fig. 1(a) and coplanar configuration in Fig. 1(c), are shown in Fig. 2 for a comparison. Here  $h$  is taken as 0.5; as evident in the figure, the lowest branch for the coplanar configuration is always lower than umbrella-type configuration. This is the reason why quantum fluctuations stabilize the coplanar configuration more.

Using these spin-wave frequencies, we have evaluated the quantum correction for the four spin configurations. The results are shown in Fig. 3; we find that quantum fluctuations favor the coplanar configuration (b) or (c). As we can see in various theoretical models,<sup>10-12)</sup> collinear spin configuration is stabilized the most by quantum fluctuations.

Note that the quantum contribution favoring the coplanar configuration is in contrast with the classical contribution of  $\Delta$ , which stabilizes more the umbrella-type configuration. Therefore in the presence of anisotropy, there must be a competition between the quantum contribution and the classical energy difference. We have evaluated the total energy

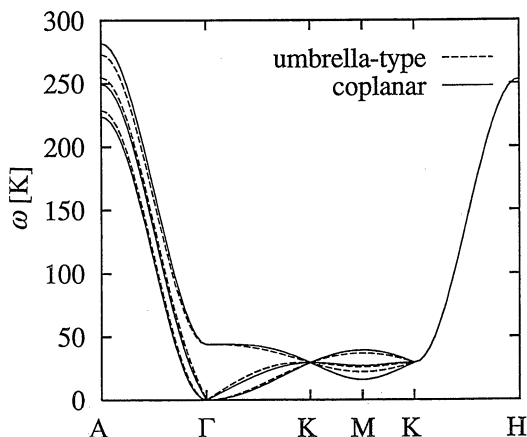


Fig. 2. Calculated spin-wave spectrum at  $h=0.5$  for the umbrella-type configuration (a) and the coplanar configuration (c).

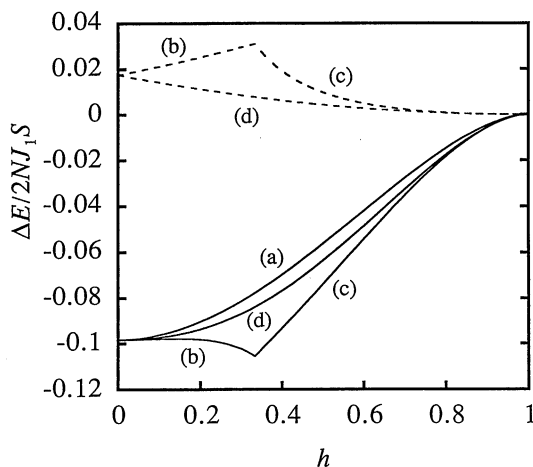


Fig. 3. The  $1/S$  correction to the ground state energy for the four spin configurations in Fig. 1. The intrachain coupling  $J_0$  and interchain coupling  $J_1$  are chosen as  $J_0=28$  K and  $J_1=4.9$  K.  $\Delta$  is assumed to be 0. The dashed line denotes the classical difference of the energy measured from the umbrella-type configuration.

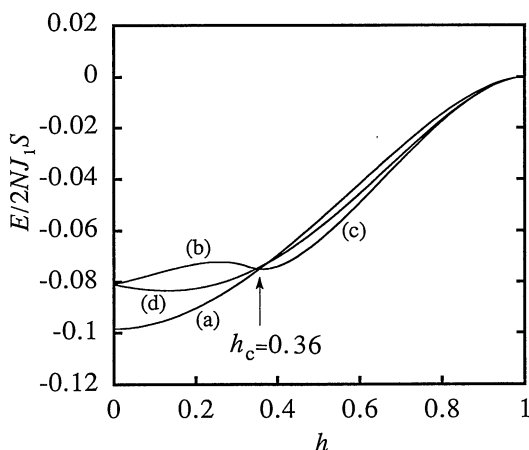


Fig. 4. The total ground-state energy for the four spin configurations, which is the sum of the  $\Delta$ -linear classical energy and the  $1/S$  quantum correction shown in Fig. 3. Here  $E$  is measured from the classical energy for the umbrella-type configuration.

by adding the classical energy linear in  $\Delta$  and the quantum correction proportional to  $1/S$ . Since  $\Delta$  is small in  $\text{CsCuCl}_3$ , we take  $\Delta=0$  in evaluating the quantum contribution. For the contribution due to the anisotropy  $\Delta$ , we take the classical value which has been calculated in §2. We have used the following values for the parameters:  $J_0=28$  K,  $J_1=4.9$  K,  $\Delta=0.07$ .

These values are very close to what Tanaka *et al.*<sup>5)</sup> used to interpret ESR data<sup>4)</sup> and they are consistent with other previous experiments.<sup>2,3)</sup> Figure 4 shows the total ground-state energy which is measured from the classical energy for the umbrella-type configuration. For  $h < h_c=0.36$ , the energy of the umbrella-like configuration is clearly lower than the coplanar-type configurations. However, the coplanar configuration (c) has the lowest energy for  $h > h_c$ . Thus we expect the spin structure to change at  $h_c$  from the umbrella-like one in Fig. 1(a) to the coplanar type in Fig. 1(c). The value of  $h_c$  is in a reasonable agreement with the experimental result,  $h_c=0.4$ . The magnitude of the magnetization jump at  $H_c$  is estimated in the classical approximation as

$$\Delta M = M_0 \Delta \frac{(1-h_c^4)}{36h_c^3}, \quad (33)$$

where  $M_0=g\mu_B S$  is the saturation magnetization. Substituting  $h_c=0.36$  and  $\Delta=0.07$  into (33), we obtain  $\Delta M=0.041M_0$ , which should be compared with the experimental value  $\Delta M=0.012M_0$ .<sup>6)</sup> At present we do not know whether this discrepancy is serious or not.

At finite temperatures, we must take into account the effect of thermal fluctuations. We have evaluated the free energy for each configuration by taking into account a contribution, which is due to the entropy of thermal spin-wave excitations. As done in evaluating the quantum contribution, we take  $\Delta=0$  in evaluating the entropy. Namely, the free energy has been calculated from the following formula:

$$F = E_0 - (2J_0 + 3J_1)NS + \frac{S}{2} \sum_{l=1}^3 \sum_k \omega_l(k) + T \sum_{l=1}^3 \sum_k \ln \left[ 1 - \exp \left\{ -\frac{S\omega_l(k)}{T} \right\} \right]. \quad (34)$$

Here we take the Boltzmann constant to be unity. Figure 5 shows the resulting free energy for various temperatures. We see that the coplanar structure (b) or (c) is the most stabilized by thermal fluctuations. Therefore we expect the critical field  $H_c$  to decrease with increasing temperature. It is qualitatively con-

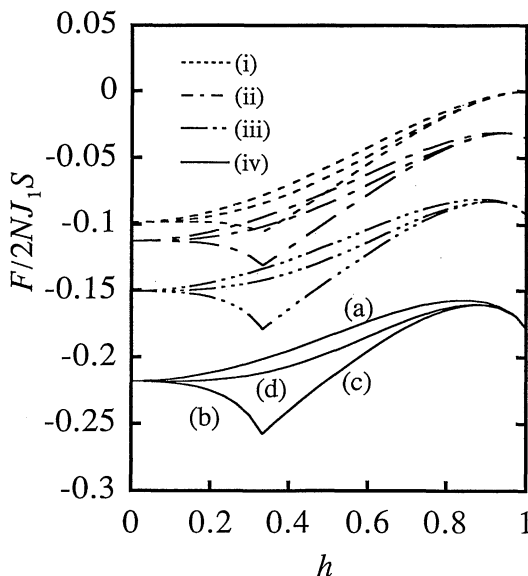


Fig. 5. The free energy for the four spin configurations which is measured from the classical ground state energy for the umbrella-type configuration. (i)  $T/2J_1S=0$  (ii)  $T/2J_1S=1.0$  (iii)  $T/2J_1S=1.5$  (iv)  $T/2J_1S=2.0$ .

sistent with the observed phase diagram in ref. 6.

#### §4. Summary and Discussion

We have shown that the small jump in magnetization of  $\text{CsCuCl}_3$  for the magnetic field applied parallel to the  $c$ -axis is likely to be due to a quantum-fluctuation-induced phase transition. The abrupt change of magnetization is explained as a spin flop transition from the umbrella-type configuration to the coplanar configuration, which is caused by the quantum effect. In the field lower than  $H_c$ , the umbrella-type structure is stabilized by the easy-plane anisotropy, while in the field higher than  $H_c$  the coplanar configuration is stabilized by quantum fluctuations. There is a competition between the easy-plane anisotropy which favors the umbrella-type configuration and quantum fluctuations which favors the coplanar configuration. In ordinary materials, the anisotropy energy is dominant over the quantum effect. However, the  $\text{Cu}^{2+}$  ion in  $\text{CsCuCl}_3$  has  $S=1/2$  and the anisotropy appears to be very weak; therefore quantum fluctuations can overcome the anisotropy in this substance. At finite temperatures, thermal fluctuations favor

more the coplanar configuration.

Let us comment on a different theoretical interpretation for the anomaly of the magnetization. Fedoseeva *et al.*<sup>14,15)</sup> suggested that the transition at  $H_c$  is caused by the dipole-dipole interaction which leads to an incommensurate magnetic structure with the long-wave modulation. However, as shown in ref. 16, the dipole-dipole interaction can cause an incommensurate state only near the Néel temperature. It seems, therefore, that their theory cannot explain the transition at low temperatures.

Recently an experimental check for our proposal has been carried out by Professor Motokawa's group, who uses the neutron scattering with a combination of pulsed neutron and pulsed magnetic field.<sup>17)</sup> Their results up to 14 T are consistent with the proposed phase transition. The phase transition at  $H_c$  has also been observed clearly by ESR<sup>18)</sup> and NMR.<sup>19)</sup>

In the present calculation, we took  $\Delta=0$  in the calculation of the quantum contribution and used the classical energy difference for the contribution of  $\Delta$ . In other words, we have kept only the lowest order in  $\Delta$  and  $1/S$ . More improved treatment is desired to take into account the quantum fluctuations for  $\Delta>0$ . It is left for a future study.

Finally we wish to discuss briefly the case of the external field perpendicular to the  $c$ -axis.<sup>20)</sup> The observed magnetization curve shows a small plateau around 12 T in this case. We speculate this plateau corresponds to the collinear configuration with one third of the saturation magnetization, which is the most stabilized by quantum fluctuations.<sup>10)</sup> In this case, however, the situation is complicated due to the broken axial symmetry. It has been shown classically that a continuous phase transition from the helical (i.e. incommensurate) state to the commensurate state occurs due to the magnetic field. Details of the study on the perpendicular case will be reported elsewhere.<sup>20)</sup>

#### Acknowledgements

We would like to express our sincere thanks to Professor M. Motokawa for showing us his unpublished experimental data and for useful discussions. We are also indebted to Dr. N. Stüßer, Professor B. Lüthi, Dr. U. Schotte and Professor K. D. Schotte for valuable dis-



cussions.

### References

- 1) K. Adachi, N. Achiwa and M. Mekata: J. Phys. Soc. Jpn. **49** (1980) 545; N. Stüßer: unpublished.
- 2) Y. Tazuke, H. Tanaka, K. Iio and K. Nagata: J. Phys. Soc. Jpn. **50** (1981) 3919.
- 3) H. Hyodo, K. Iio and K. Nagata: J. Phys. Soc. Jpn. **50** (1981) 1545.
- 4) W. Palme, F. Mertens, O. Born, B. Lüthi and U. Schotte: Solid State Commun. **76** (1990) 873.
- 5) H. Tanaka, U. Schotte and K. Schotte: J. Phys. Soc. Jpn. **61** (1992) 1344.
- 6) M. Motokawa: presented at the Annual Meeting of the Phys. Soc. Jpn. (1978); H. Nojiri, Y. Tokunaga and M. Motokawa: *Proc. Int. Conf. Magnetism, Paris, 1988*, J. Phys. (Paris) **49** (1988) Suppl. C8, p. 1459.
- 7) S. Hirotsu: J. Phys. C**10** (1977) 967.
- 8) H. Kawamura: J. Phys. Soc. Jpn. **53** (1984) 2452.
- 9) H. Kawamura and S. Miyashita: J. Phys. Soc. Jpn. **54** (1985) 4530.
- 10) A. V. Chubukov and D. I. Golosov: J. Phys. C**3** (1991) 69.
- 11) T. Oguchi, H. Nishimori and Y. Taguchi: J. Phys. Soc. Jpn. **54** (1985) 4492.
- 12) K. Kubo and T. Kishi: J. Phys. Soc. Jpn. **60** (1991) 567.
- 13) H. Shiba and T. Nikuni: *Recent Advances in Magnetism of Transition Metal Compounds*, ed. A. Kotani and N. Suzuki (World Scientific, 1993) p. 372.
- 14) N. V. Fedoseeva, R. S. Gekht, T. A. Velikanova and A. D. Balaev: JETP Lett. **41** (1985) 408.
- 15) R. S. Gekht, N. V. Fedoseeva, V. A. Dolina and A. D. Balaev: Phys. Status Solidi (b) **155** (1989) 639.
- 16) H. Shiba and N. Suzuki: J. Phys. Soc. Jpn. **51** (1982) 3488.
- 17) M. Mino, K. Ubukata, T. Bokui, M. Arai, H. Tanaka and M. Motokawa: preprint.
- 18) H. Ohta, S. Imagawa, M. Motokawa, and H. Tanaka: to appear in J. Phys. Soc. Jpn.
- 19) M. Chiba, K. Ohara, Y. Ajiro and T. Morimoto: presented at the Annual Meeting of the Phys. Soc. Jpn. (1993).
- 20) A. E. Jacobs, T. Nikuni and H. Shiba: submitted to J. Phys. Soc. Jpn.